Climate change impact on peak discharge characteristics of the Whanganui River at Anzac Parade

An analysis of river discharge at Anzac Parade under different warming scenarios

Prepared for Horizons Regional Council

May 2022

Prepared by:
Christian Zammit

For any information regarding this report please contact:

Christian Zammit
Hydrologist
Hydrological Modelling Group

+64-3-343 7879
christian.zammit@niwa.co.nz

National Institute of Water & Atmospheric Research Ltd
PO Box 8602
Riccarton
Christchurch 8011

Phone +64 3 348 8987

Revision	Description	Date
Version 1.0	Final Report	27 May 2022

Quality Assurance Statement		
signature	Reviewed by:	Dr James Griffiths
signature	Formatting checked by:	Rachel Wright
signature	Approved for release by:	Phillip Jellyman

Contents

Tables

Figures

1   Introduction

NIWA was engaged by Horizons Regional Council (HRC) to assess the potential impact of climate change on the hydrological characteristics of the Whanganui River at Anzac Parade. This information is needed by HRC for part of a review of the Whanganui River flood risk under climate change and for community consultation.

The question HRC needs to answer is how climate change will affect the flood risk in the 2050–2100 timeframe. Specifically, HRC is seeking climate change analysis based on flow estimates for the 1 in 50, 1 in 100, and 1 in 200-year Annual Return Interval (ARI) events, corresponding respectively to 2%, 1%, 0.5% Annual Exceedance Probabilities (AEP). The flow estimates are to be provided at 20, 50 and 100-year timeframes to enable HRC to discuss incremental changes with residents; as well as across all warming scenarios characterised by Representative Concentration Pathways (RCPs) to explore implications of the different RCP scenarios with residents.

2   Methodology

As agreed with HRC, the following methodology was used to develop an understanding of the potential impact of climate change on flood characteristics of the Whanganui River at Anzac Parade using hydrological simulations completed as part of the Deep South National Science Challenge (DSC) project "Climate impact on the national water cycle" (referred hereafter as the 'Deep South project'). As part of the DSC project, NIWA coupled climate change projections (Ministry for Environment 2018, referred hereafter as NZ climate projections) with NIWA's national hydrological modelling tool, TopNet (Clark et al. 2008), to generate hydrological simulations across 43,000 river reaches in New Zealand. Modelling was performed for four radiative forcing scenarios (the previously mentioned 'Representative Concentration Pathways', RCPs), using data from six climate models[1] (Global Circulation Models, GCMs), and run over the 128-year period 1971–2099. For simplicity and to primarily isolate the climate change effect, it was assumed that land use remained the same over the entire period of simulation. As part of this project we are proposing to leverage simulations and existing post-processing (from hourly to daily time step), which were carried out as part of the Deep South project.

The following methodology was used to assess the potential impact of climate change on flood risk for the Whanganui at Anzac Parade.

- Flood risk is calculated under a stationarity assumption assuming a Gumbel distribution of peak daily discharge.

- Flood risk is characterised by change to the 1:50, 1:100 and 1:200 ARI flow events across different time slices and emission scenarios assuming only riverine discharge (i.e., the rivers remain within the confine of the river channel system).

- Due to the hydrological and climate model assumptions, flood risk is reported as an absolute figure, and as change to reference scenario (1985-2006). As the hydrological model used was uncalibrated, it is recommended that only the change analysis is used to inform discussions with community.

- Changes in flood risk are characterised over 20 year running periods for 2040s (2030–2049), 2050s (2040–2059), 2060s (2050–2069), 2070s (2060-2079), 2080s (2070–2089) and 2090s (2080–2098).

- To better quantify the uncertainties associated with the projection of flood risk, three assessment methods are implemented:

  – Extreme event analysis is carried out on the 20 year periods of interest only. This analysis aligns with the fifth IPCC assessment report (AR5) (IPCC 2014) recommendation regarding climate change impact[2].

  – Extreme event analysis is carried out starting from 2006 to the period of interest. This analysis focuses only on the IPCC 5th Assessment's future time period and assumes stationarity over that period.

  – Extreme event analysis is carried out with all the information starting in 1986 (i.e., including the hindcast period to the period of interest). This analysis is similar to

---

[1] Information on the NZ climate projections in Section 3.
[2] Information associated with IPCC 6th Assessment is not available before 2024.

the current methodology in used by regional council, for which the longest possible annual time series is considered under stationarity assumption.

Assessment of climate change on flood risk is generally carried out for a specific GCM (for physical consistency) or for a pool of GCMs (each GCM is considered equally possible). Existing literature on climate change impact on flood risk does not recommend any specific methodological choice for assessment of climate change impact on flood risk. From an uncertainty point of view, GCM specific assessment tends to carry larger uncertainty than pooled GCM assessment due to the reduced sample size available for extreme event analysis. From a physics point of view, GCM specific comparison tends to respect physical differences between GCMs and their associated projections (similar to the concept of "comparing apples with apples"). This enables a direct representation of climate change effects independently of the GCM properties.

3   Climate change projections

Based on the fifth Intergovernmental Panel on Climate Change (IPCC) assessment report (AR5) (IPCC 2014), NIWA assessed up to 41 GCMs from the AR5 model archive (referred to hereafter as the Coupled Model Intercomparison Project version 5 (CMIP5)) for their suitability to the New Zealand region. Validation of the GCMs was carried out by comparison against large scale climate and atmospheric circulation characteristics using 62 metrics (Ministry for the Environment 2018). This analysis provided performance-based ranking relative to New Zealand's historical climate. Six GCMs were chosen as being best at representing climatic dynamics around New Zealand and for spanning a useful range of climate change sensitivities to CO_2 projections. The six CMIP5 models selected were:

- HadGEM2-ES (Jones et al. 2011).

- CESM1-CAM5 (Meehl et al. 2013).

- NorESM1-M (Bentsen et al. 2013).

- GFDL-CM3 (Griffies et al. 2011).

- GISS-E2-R (Schmidt et al. 2014).

- BCC-CSM1.1 (Wu et al. 2014).

The GCMs were driven by four scenarios of future emissions of greenhouse gases and aerosols (RCPs), and by data representing natural processes (including solar irradiance) and historical emissions. They were otherwise unconstrained by historical climate observations. GCM outputs (i.e., atmospheric boundary condition variables and Sea Surface Temperature, SST) were then used to drive a Regional Climate Model (RCM) to refine the variables to a more useful spatial scale for the country (29 km resolution). The output of the regional climate modelling (referred hereafter as NZ projections) were dynamical downscaling (Sood 2014) and rudimentary bias correction to 0.05 degrees resolution (~5 km) for use across New Zealand and became the input for hydrological modelling. Further details on the validation and GCM and RCM modelling can be found in Sood (2014) and Ministry for the Environment (2018).

The downscaled climate data used in this study ran from 1971 to 2100. From 2005 onward, as per IPCC recommendations, each GCM was driven by four RCPs that encapsulate alternative scenarios of radiative forcing and reflect alternative trajectories of global societal behaviour with regard to greenhouse gas emissions and other activities. The range of RCPs used can help shed light on the utility of climate change mitigation. Descriptions and trajectories of the four RCPs are provided in Table 3-1 and Figure 3-1. By mid-century, the temperature trajectory of RCP2.6 is the coolest and RCP8.5 the warmest, with RCP4.5 and RCP6.0 producing intermediate warming. While RCP6.0 ends the century with more forcing than RCP4.5, early and mid-century it is RCP4.5 that has higher greenhouse gas emissions and a stronger radiative forcing; this is somewhat reflected by the mid-century temperature change ranges for the New Zealand seven-station network (Table 3-1). RCP6.0 overtakes RCP4.5 after the middle of the century.

It is important to note that the climatic and hydrological effects of the RCPs are not a linear or monotonic progression from the lowest to highest RCP. Furthermore, the spatial patterns of climatic change across New Zealand vary for different combinations of RCP and RCM simulations.

Table 3-1:   **Descriptions of the Representative Concentration Pathways (RCPs).** Temperature changes are the GCM mean (°C) and, in brackets, the likely ranges.

Representative Concentration Pathway	Description	Seven-station temperature change (Ministry for the Environment 2018)		Global surface temperature change for 2081–2100 (IPCC 2014, Table 2.1)
		2031-2050	2081-2100	
RCP2.6	The least change in radiative forcing considered, by the end of the century, with +2.6 W/m^2 by 2100 relative to pre-industrial levels.	0.7 (0.2 - 1.3)	0.7 (0.1 - 1.4)	1.0 (0.3 - 1.7)
RCP4.5	Low-to-moderate change in radiative forcing by the end of the century, with +4.5 W/m^2 by 2100 relative to pre-industrial levels	0.8 (0.4 - 1.3)	1.4 (0.7 - 2.2)	1.8 (1.1 - 2.6)
RCP6.0	Moderate-to-high change in radiative forcing by the end of the century, with +6.0 W/m^2 by 2100 relative to pre-industrial levels.	0.8 (0.3 - 1.1)	1.8 (1.0 - 2.8)	2.2 (1.4 - 3.1)
RCP8.5	The largest change in radiative forcing considered, by the end of the century, with +8.5 W/m^2 by 2100 relative to pre-industrial levels.	1.0 (0.5 - 1.7)	3.0 (2.0 - 4.6)	3.7 (2.6 - 4.8)
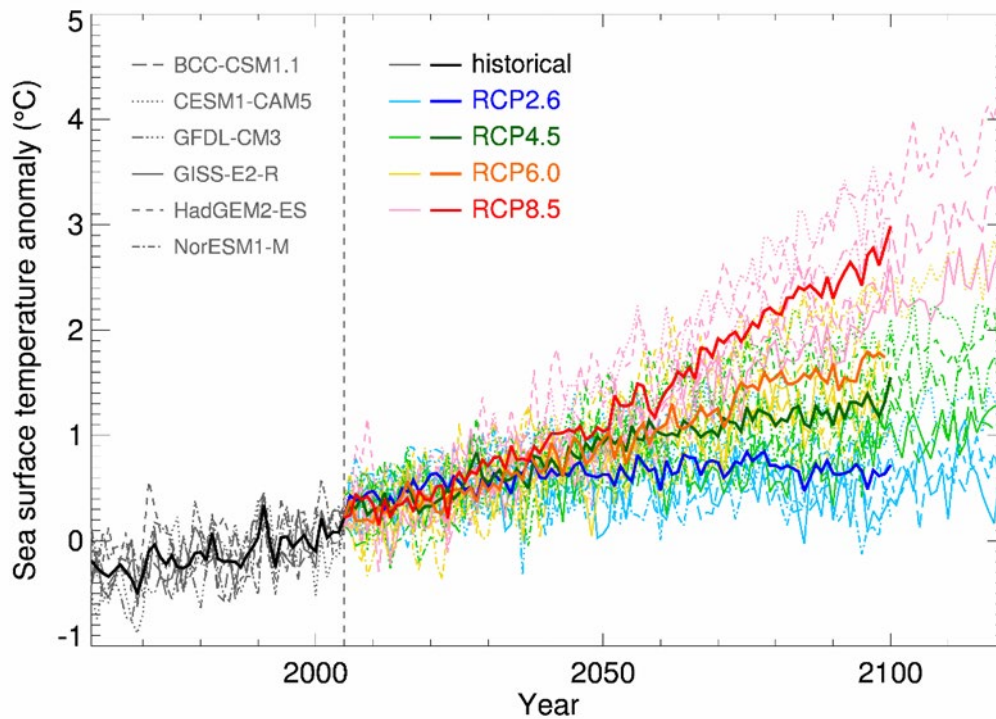
Figure 3-1: **CMIP5 global climate models (2006–2120) and historical simulations (1950-2006).** Bias-adjusted SSTs, averaged over the RCM domain, for 6 (1960–2005), and four future simulations (RCPs 2.6, 4.5, 6.0 and 8.5), relative to 1986–2005. Individual models are shown by thin dotted, dashed or solid lines (shown in grey in the inset legend), and the six-model ensemble-average by thicker solid lines, all of which are coloured according to the RCP pathway.

4   Hydrological model - TopNet

The catchment hydrological model used in this study is NIWA's TopNet model (Clark et al. 2008), which is routinely used for surface water hydrological modelling applications in New Zealand. It is a spatially semi-distributed, time-stepping model of water balance. It is driven by time-series of precipitation and temperature, and additional weather elements where available. TopNet simulates water storage in the snowpack, plant canopy, rooting zone, shallow subsurface, lakes and rivers. It produces a time-series of modelled river flow (without consideration of water abstraction, impoundments, or discharges) throughout a modelled river network, and evapotranspiration (derived from weather/climate input information) but does not adjust river flows for effects of irrigation. TopNet has two major components, namely a catchment module and a flow routing module.

The model combines TOPMODEL hydrological model concepts (Beven et al. 1995), a kinematic wave channel routing algorithm (Goring 1994), and a simple temperature based empirical snow model (Clark et al. 2008). As a result, TopNet can be applied across a range of temporal and spatial scales by using small sub-basins as model elements (Ibbitt and Woods 2002; Bandaragoda et al. 2004). Considerable effort has been made during the development of TopNet to ensure that the model has a strong physical basis and that the dominant rainfall-runoff dynamics are adequately represented. TopNet model equations and information requirements are given in Clark et al. (2008) and McMillan et al. (2013). The version of the model used in this project does not consider water transfers between catchments or other water storages and does not model aquifer water balances. It is similar to the hydrological model used by NIWA for short term flood forecasting risk across New Zealand (McMillan et al. 2013).

For the development of the national-scale version of the TopNet model used in this study, spatial information was provided by national datasets including:

- Catchment topography based on a nationally available 30 m Digital Elevation Model (DEM).

- Physiographical data based on the Land Cover Database (version 3, LCDB3) and Land Resource Inventory (Newsome et al. 2000).

- Soil data based on the Fundamental Soil Layer information (Newsome et al. 2000).

- Hydrological properties (based on the River Environment Classification version 2.3, REC2.3) (Snelder and Biggs 2002)[3].

The method for deriving TopNet parameters based on the above data sources is given in Table 1 of Clark et al. (2008). Due to the paucity of some spatial information at national/regional scale, some soil parameters are set uniformly across New Zealand.

TopNet is currently configured to use LCDB3 (Newsome et al. 2000), reflecting 2008 land cover (rather than the latest version (version 5), which corresponds to 2016 landcover data). There are differences in land use between the two, and these may have hydrological consequences. However, they are likely to be small in comparison with changes up to 2100. During the course of the simulations from 1971 to 2100, land use is kept constant. The purpose of this is to isolate the effects

---

[3] For sake of consistency, landcover and soil information were kept consistent with previous study (Collins and Zammit 2016)

of changing climate on the hydrological response (incorporating land use changes would confound interpretation of the results).

Hydrological simulations used the REC 2 digital network (version 3) aggregated up to Strahler[4] order three (approximate area 7 km^2) and this is the same process that was used within previous national and regional scale assessments There were some situations (e.g., residual coastal catchments) where smaller stream orders were not subsumed into larger catchments for the hydrological simulations. The simulation results consist of hourly time-series of hydrological variables for each computational sub-catchment and were produced for the six GCMs and four RCPs considered.

Soil and land use characteristics within each computational sub-catchment are homogenised for use in the TopNet model. This means that the soil characteristics and physical properties of different land use, such as pasture and forest, will be spatially averaged, and the hydrological model outputs will be an approximation of conditions across land uses.

To conduct the simulations required for this study, TopNet was run continuously for the period 1971 to 2099, with the spin-up year 1971 excluded from the analysis. The climate inputs were stochastically disaggregated from daily to hourly data. As the GCM simulations are based only on initial conditions and not updated with observational data, comparison between present and future hydrological conditions can be made directly (as each GCM is characterised by specific physical assumptions and parameterisation). However, this means that hindcasts hydrological simulations will not track observational data.

---

[4] Strahler order describes river size based on tributary hierarchy. Headwater streams with no tributaries are order 1; 2nd order streams develop at the confluence of two 1st order tributaries; stream order increases by 1 where two tributaries of the same order converge.

5　Climate change impact on flood characteristics

Hydrological characterisation of floods generally requires flood frequency analysis (FFA) to be conducted using annual peak discharge time series, calculated as the annual time series of maximum discharge at the location of interest. To measure the effect of climate change on flood risk, simulated data from the 20 years baseline period (mid-1985 to mid-2006) are compared to a three-member ensemble of six future time periods:

- 2040s (2030–2049), 2050s (2040–2059), 2060s (2050–2069), 2070s (2060–2079),2080s (2070–2089) and 2090s (2080–2098) on which FFA is performed using the 20-year period of interest data only (in line with climate change assessment methodology). This is referred hereafter as the "20 years analysis".

- 2040s (2006-2049), 2050s (2006-2059), 2060s (2006-2069), 2070s (2006-2079),2080s (2006-2089) and 2090s (2006-2098) on which FFA is performed on data starting from 2006 to the end of the 20 year period of interest (i.e., FFA estimated over the whole future period). This is referred hereafter as the "From 2006 analysis".

- 2040s (1986–2049), 2050s (1986–2059), 2060s (1986–2069), 2070s (1986–2079), 2080s (1986–2089) and 2090s (1986–2098) on which FFA is performed on data starting from 1986 to the end of the 20-year period of interest (i.e., FFA performed using the longest annual time series; current methodology used by regional council). This is referred hereafter as the "From 1986 analysis".

The numbered year indicates calendar year starting on January 1 and ending on December 31. The last period (i.e., 2090s) is shifted a year earlier relative to the 2040s because climate simulations end before 31 December 2099 for HadGEM-2 GCM under RCP 6.0. The magnitude of the climate change effect on peak flood magnitude is determined by the difference between the simulated peak flood magnitudes calculated over the baseline and future periods.

The assessment of climate change on flood risk is presented hereafter using two methodologies: i) GCM specific (for each of the six GCMs) analysis; or a pool of GCMs (see Section 2). GCM specific assessment tends to carry larger uncertainty than pooled GCM assessment, due to the smaller sample size available for extreme event analysis.

5.1　Annual time series analysis

Figure 5-1 and Figure 5-2 present the simulated annual maximum daily discharge time series for each GCM for each radiative forcing scenario, over the whole period of simulation (1986–2098).
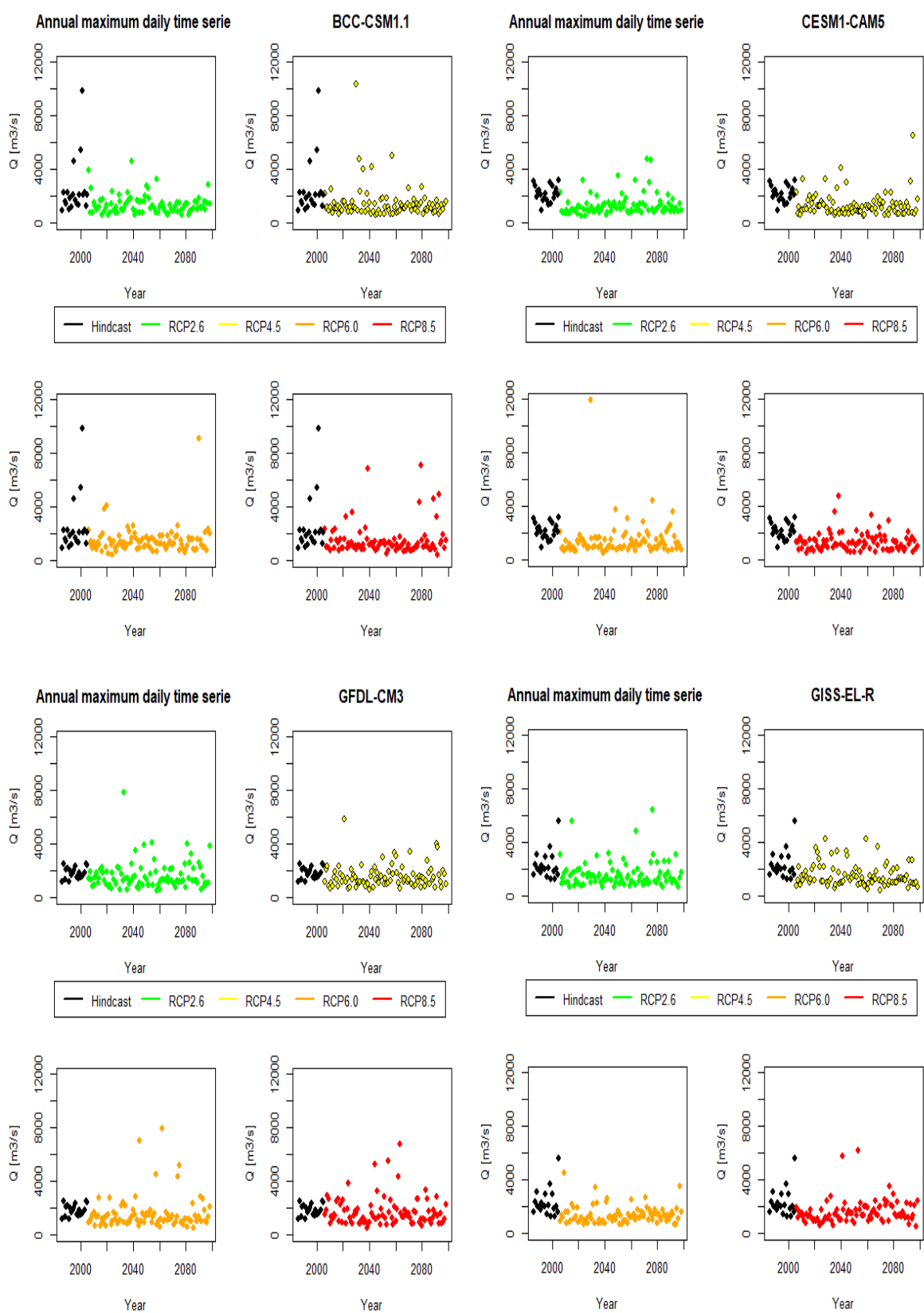
Figure 5-1: **Simulated annual maximum daily discharge for the period 1986-2098 under four radiative forcing scenarios for GCMs: BCC-CSM1.1 (top left); CESM1-CAM5 (top right); GFDL-CM3 (bottom left); and GISS-EL-R (bottom right).** Annual maximum daily discharge over the hindcast period (black dots), RCP2.6 (green dots), RCP4.5 (yellow dots), RCP6.0 (orange dots) and RCP8.5 (red dots).
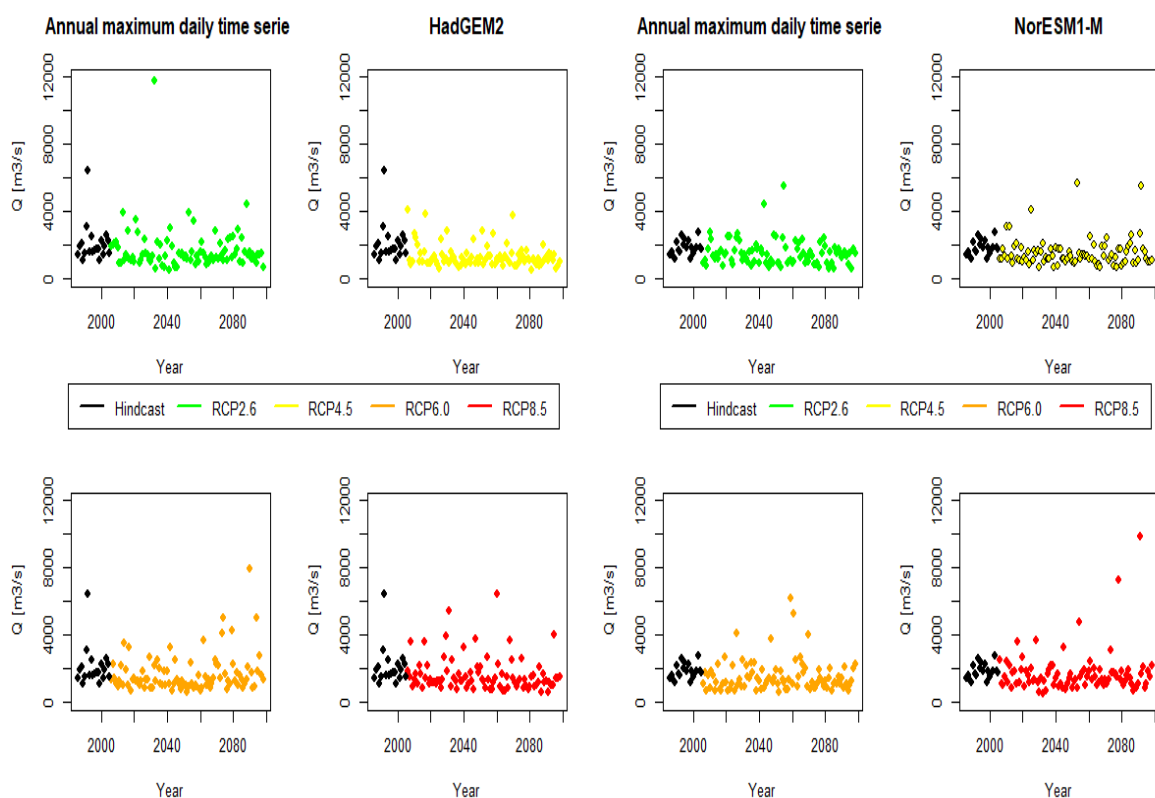
Figure 5-2: **HadGEM2 (left) and NorESM1-M (right) GCM driven simulated annual maximum daily discharges over the period 1986-2098 under four radiative forcing scenarios .** Annual maximum daily discharge over the hindcast period (black dots), RCP2.6 (green dots), RCP4.5 (yellow dots), RCP6.0 (orange dots) and RCP8.5 (red dots).

Analysis of the annual time series indicates that:

- There is large variation in magnitude and timing of annual maxima in the daily discharge time series between each GCM.

- There is no consistent correlation (qualitative assessment) between simulated annual maximum discharge and time. As a result, extreme annual discharge is not expected to get more extreme with time as expected following IPCC AR5 conclusions (IPCC 2014).

- There is no consistent correlation (qualitative assessment) between simulated annual maximum discharge and radiative forcing scenario. As a result, extreme annual discharge is not expected to get more extreme with radiative forcing as expected following IPCC AR5 conclusions (IPCC 2014).

The above results were expected because of the way the NZ projection ensemble has been developed (see Ministry for the Environment 2018). They reflect the change in weather patterns expected under climate change. No attempt has been made (in this project) to carry out such analysis at seasonal time scale.

5.2 Flood Frequency Analysis

Flood frequency analysis was carried out on the GCM driven annual maximum discharge time series under a stationarity assumption and assuming a Gumbel distribution of peak daily discharge. Flood

risk was characterised for the 1:50, 1:100 and 1:200-year ARI flow events across different time slices and emission scenarios assuming only riverine discharge (i.e., the rivers remain within the confine of the river system). For clarity, the results presented hereafter (for the future time period analysis) are for the pooled GCM result (referred to as GCM ensemble hereafter). This was done because the pooled GCM analysis has lower uncertainty bounds (due to its sample size) than GCM specific analysis. GCM specific results are available in Appendix A–C . All analysis was carried out using the "extreme" package in R assuming a Gumbel distribution.

5.2.1   Hindcast Flood Frequency Analysis

Table 5-1 presents the results of the GCM specific FFA carried out for the 1:50, 1:100 and 1:200-year ARI daily maximum discharge event associated with the corresponding 95% confidence interval, while Figure 5-3 provides a continuous representation of the FFA between the 1:2 and 1:200-year ARI event.

Table 5-1:   **Hindcast GCM driven flood frequency analysis (m^3/s) for the Whanganui River at Anzac Parade.** 95th percentile confidence interval provided in brackets.

	Return period		
GCM	**1:50 year ARI**	**1:100 year ARI**	**1:200 year ARI**
HadGEM2-ES	3848 [2987 - 4709]	4232 [3239 - 5225]	4615 [3488 - 5741]
CESM1-CAM5	4157 [3285 - 5029]	4558 [3558 - 5558]	4958 [3830 - 6087]
GFDL-CM3	3081 [2552 - 3639]	3334 [2693 - 3975]	3589 [2862 - 4310]
GISS-EL-R	4204 [3282 - 5125]	4612 [3549 - 5674]	5018 [3814 - 6222]
BCC-CSM1.1	5378 [3841 - 6916]	6028 [4250 - 7806]	6675 [4655 - 8695]
NorESM1-M	3119 [2533 - 3705]	3383 [2709 - 4056]	2646 [2384 - 4407]
Ensemble	3983 [3616 - 4350]	4382 [3959 - 4805]	4780 [4300 - 5216]
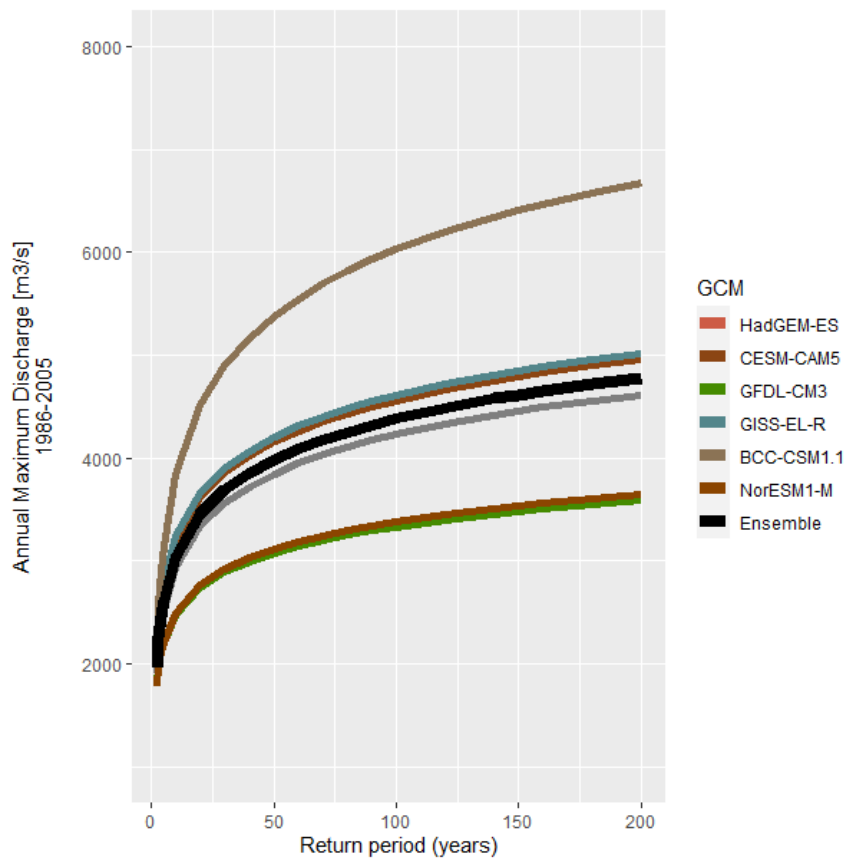
Figure 5-3:   Hindcast GCM driven flood frequency .   Fore sake of simplicity confidence interval associated with FFA are not represented.

Analysis of the GCM driven FFA indicates:

- There is a large variation (approximately a factor of two) in the range of flood characteristics across GCMs.

- Depending on the GCM, uncertainty bounds associated with flood characteristics reaching up to 50% of the flood characteristic (e.g., BCC-CSM1.1 1:200-year ARI).

5.2.2   20 years analysis

Hydrological characterisation of floods generally requires FFA to be conducted using annual peak discharge time series , calculated as the annual time series of maximum discharge at the location of interest. To measure the effect of climate change on flood risk, simulated data from the 20-year baseline period (mid-1985 to mid-2006) are compared to six 20-year centred future time periods: 2040s (2030–2049), 2050s (2040–2059), 2060s (2050–2069), 2070s (2060–2079), 2080s (2070–2089) and 2090s (2080–2098) on which FFA is performed. This is referred as the "20 years analysis".

Table 5-2 presents pooled GCM FFA analysis, for all time periods of interest, carried out for the 1:50, 1:100 and 1:200-year ARI daily maximum discharge events and the corresponding 95% confidence interval under the four radiative forcing pathways.

Table 5-2: **20 years pooled GCM FFA analysis and associated 95th percentile uncertainty across radiative forcing pathways over the period 2040s–2090s.** FFA calculated on annual peak discharge (m³/s) over 20 years' time period centred on the period of interest.

	2030-2049	2040-2059	2050-2069	2060-2079	2070-2089	2080-2098
1:50-year ARI						
RCP 2.6	3420 [3041 - 3798]	3417 [3037 - 3795]	3190 [2849 - 3529]	3030 [2714 - 3344]	3315 [2960 - 3669]	3015 [2709 - 3320]
RCP 4.5	3201 [2842 - 3558]	3102 [2769 - 3435]	2921 [2624 - 3217]	2764 [2497 - 3030]	2729 [2462 - 2995]	2941 [2624 - 3258]
RCP 6.0	3105 [2779 - 3429]	3010 [2690 - 3329]	3100 [2773 - 3425]	3547 [3156 - 3986]	3066 [2746 - 3384]	3260 [2903 - 3616]
RCP 8.5	3402 [3028 - 3774]	3332 [2976 - 3687]	3574 [3188 - 3959]	3754 [3333 - 4173]	3229 [2881 - 3576]	3235 [2883 - 3585]
1:100-year ARI						
RCP 2.6	3820 [3383 - 4257]	3813 [3375 - 4250]	3546 [3153 - 3987]	3360 [2996 - 3724]	3687 [3277 - 4096]	3338 [2986 - 3690]
RCP 4.5	3572 [3158 - 3985]	3452 [3067 - 3836]	3239 [2896 - 3580]	3055 [2710 - 3311]	3017 [2710 - 3324]	3266 [2900 - 3632]
RCP 6.0	3446 [3071 - 3820]	3344 [2975 - 3713]	3444 [3068 - 3820]	3953 [3502 - 4403]	3404 [3035 - 3771]	3628 [3215 - 4039]
RCP 8.5	3794 [3363 - 4225]	3709 [3297 - 4119]	3985 [3539 - 4430]	4193 [3708 - 4678]	3592 [3190 - 3993]	3599 [3194 - 4003]
1:200-year ARI						
RCP 2.6	4219 [3722 - 4714]	4209 [3712 - 4704]	3900 [3455 - 4345]	3690 [3286 - 4102]	4058 [3592 - 4522]	3661 [3262 - 4058]
RCP 4.5	3942 [3472 - 4411]	3801 [3364 - 4237]	3554 [3166 - 3942]	3346 [2998 - 3692]	3305 [2957 - 3652]	3590 [3175 - 4005]
RCP 6.0	3787 [3362 - 4211]	3678 [3259 - 4096]	3788 [3360 - 4214]	4358 [3846 - 4869]	3740 [3322 - 4158]	3994 [3526 - 4461]
RCP 8.5	4186 [3696 - 4675]	4084 [3618 - 4529]	4394 [3889 - 4899]	4632 [4081 - 5182]	3954 [3497 - 4409]	3962 [3502 - 4420]

FFA analysis across all radiative forcing scenarios for the different return period indicates:

- Future flood frequency characteristics are peaking early in the century (by the 2050's at the latest) under lowest radiative forcing pathways, while peaking by the 2070's for higher radiative forcing pathways.

- End of century 1:50-year ARI flood characteristics tend to be lower than earlier in the century indicating a change in the frequency of more common flood events at Anzac Parade. More extreme event flood characteristics tend to peak later in the century but not at the end of the century.

- Considering uncertainty, annual peak flood magnitude across future time slices and warming scenarios remain stable within 95th percentile uncertainty bands.

- Future flood frequency characteristics tends to be lower than hindcast characteristics, indicating that current level of flood risk at Anzac Parade is unlikely to change (based on a 20-year centred analysis.

5.2.3 2006 analysis

Hydrological characterisation of floods generally requires FFA to be conducted using annual peak discharge time series. To measure the effect of climate change on flood risk, simulated data from the 20 years baseline period (mid-1985 to mid-2006) are compared to six future time periods: 2040s (2006–2049), 2050s (2006–2059), 2060s (2006–2069), 2070s (2006–2079), 2080s (2006–2089) and 2090s (2006–2098) on which FFA is performed on data starting from 2006 to the end of the 20 year period of interest (i.e., FFA estimated over the whole future period starting in 2006). This is referred as the "2006 analysis". Table 5-3 presents pooled GCM FFA analysis, for all time periods of interest, carried out for the 1:50, 1:100 and 1:200-year ARI daily maximum discharge event associated with the corresponding 95% interval confidence under the four radiative forcing pathways.

Table 5-3: **2006 pooled GCM FFA analysis and associated 95th percentile uncertainty across radiative forcing pathways over the period 2040s–2090s.** FFA calculated on annual peak discharge (m^3/s) over time period starting in 2006.

	2030-2049	2040-2059	2050-2069	2060-2079	2070-2089	2080-2098
1:50-year ARI						
RCP 2.6	3277 [3039 - 3514]	3338 [3116 - 3558]	3253 [3057 - 3447]	3258 [3075 - 3440]	3267 [3095 - 3437]	3210 [3052 - 3367]
RCP 4.5	3193 [2961 - 3424]	3206 [2995 - 3416]	3108 [2924 - 3291]	3078 [2910 - 3246]	3013 [2860 - 3165]	3051 [2902 - 3199]
RCP 6.0	3052 [2834 - 3270]	3007 [2813 - 3200]	3067 [2886 - 3247]	3158 [2982 - 3333]	3067 [2909 - 3224]	3179 [3021 - 3336]
RCP 8.5	3228 [2998 - 3457]	3263 [3053 - 3473]	3339 [3140 - 3536]	3396 [3206 - 3586]	3312 [3140 - 3484]	3361 [3194 - 3528]
1:100-year ARI						
RCP 2.6	3651 [3376 - 3925]	3721 [3465 - 3975]	3622 [3396 - 3786]	3628 [3417 - 3838]	3636 [3438 - 3832]	3570 [3388 - 3752]
RCP 4.5	3553 [3285 - 3819]	3568 [3324 - 3811]	3454 [3241 - 3666]	3420 [3226 - 3613]	3344 [3168 - 3519]	3389 [3218 - 3560]

	2030-2049	2040-2059	2050-2069	2060-2079	2070-2089	2080-2098
RCP 6.0	3393 [3141 - 3644]	3341 [3118 - 3564]	3408 [3199 - 3616]	3512 [3309 - 3714]	3407 [3225 - 3588]	3537 [3354 - 3718]
RCP 8.5	3588 [3323 - 3852]	3629 [3386 - 3870]	3715 [3485 - 3943]	3782 [3562 - 4001]	3685 [3486 - 3883]	3742 [3549 - 3934]
1:200-year ARI						
RCP 2.6	4024 [3712 - 4334]	4102 [3813 - 4391]	3989 [3733 - 4244]	3996 [3757 - 4235]	4003 [3780 - 4226]	3929 [3722 - 4134]
RCP 4.5	3911 [3607 - 4213]	3929 [3653 - 4204]	3799 [3558 - 4039]	3760 [3540 - 3978]	3674 [3474 - 3873]	3726 [3531 - 3919]
RCP 6.0	3732 [3446 - 4017]	3675 [3421 - 3928]	3748 [3511 - 3984]	3866 [3636 - 4095]	3746 [3540 - 3952]	3893 [3686 - 4098]
RCP 8.5	3947 [3646 - 4246]	3993 [3718 - 4267]	4090 [3829 - 4349]	4166 [3917 - 4415]	4056 [3830 - 4280]	4121 [3902 - 4339]

FFA analysis across all radiative forcing scenarios for the different return period indicates:

- 1:50-year ARI future flood frequency characteristics are peaking by the 2050's under lowest radiative forcing pathways, while remaining stable for future time periods. Under increased warming 1:50-year ARI flood characteristics are peaking around the 2070s and remain relatively stable for future time period and with warming scenarios.

- 1:100 and 1:200-year ARI flood characteristics are peaking early in the century for the lower radiative forcing pathways and by the 2070's for higher radiative forcing pathways.

- Considering uncertainty, flood characteristics across future time slice and warming scenarios remain stable within 95th percentile uncertainty bands.

- Future flood frequency characteristics tends to be lower than hindcast characteristics (including 95th percentile uncertainty bounds), indicating that current level of flood risk at Anzac Parade is unlikely to change (based on an analysis over the full range of future time periods, i.e., starting in 2006).

5.2.4 1986 analysis

Hydrological characterisation of floods generally requires FFA to be conducted using annual maximum discharge time series. To measure the effect of climate change on flood risk, simulated data from the 20 year baseline period (mid-1985 to mid-2006) are compared to an ensemble of six future time periods: 2040s (1986–2049), 2050s (1986–2059), 2060s (1986–2069), 2070s (1986–2079), 2080s (1986–2089) and 2090s (1986–2098) on which FFA is performed on data starting from 1986 to the end of the 20 years period of interest (i.e., FFA performed using the longest annual time series; current methodology in used by regional council) . This is referred as the "1986 analysis". Table 5-4 presents pooled GCM FFA analysis, for all time periods of interest, carried out for the 1:50,

1:100 and 1:200-year ARI daily maximum discharge event associated with the corresponding 95% confidence interval under the four radiative forcing pathways.

Table 5-4: **1986 pooled GCM analysis FFA analysis and associated 95th percentile uncertainty across radiative forcing pathways over the period 2040s–2090s.** FFA calculated on annual peak discharge (m³/s) over time periods starting in 1986.

	2030-2049	2040-2059	2050-2069	2060-2079	2070-2089	2080-2098
1:50-year ARI						
RCP 2.6	3705 [3484 - 3925]	3696 [3489 - 3902]	3591 [3404 - 3778]	3564 [3387 - 3740]	3542 [3375 - 3707]	3472 [3317 - 3627]
RCP 4.5	3649 [3431 - 3867]	3606 [3404 - 3806]	3488 [3306 - 3669]	3429 [3261 - 3596]	3344 [3189 - 3497]	3352 [3202 - 3501]
RCP 6.0	3567 [3355 - 3779]	3477 [3284 - 3669]	3464 [3283 - 3463]	3489 [3317 - 3661]	3387 [3229 - 3544]	3452 [3296 - 3607]
RCP 8.5	3650 [3436 - 3864]	3623 [3424 - 3820]	3637 [3449 - 3824]	3653 [3472 - 3832]	3564 [3398 - 3729]	3585 [3424 - 3745]
1:100-year ARI						
RCP 2.6	4129 [3875 - 4382]	4121 [3882 - 4358]	4001 [3785 - 4217]	3971 [3767 - 4174]	3945 [3753 - 4136]	3865 [3685 - 4043]
RCP 4.5	4064 [3812 - 4314]	4016 [3784 - 4248]	3882 [3672 - 4090]	3816 [3622 - 4008]	3718 [3540 - 3895]	3729 [3556 - 3900]
RCP 6.0	3972 [3825 - 4331]	3872 [3649 - 4094]	3856 [3648 - 4063]	3886 [3686 - 4084]	3769 [3587 - 3950]	3844 [3664 - 4022]
RCP 8.5	4060 [3813 - 4307]	4031 [3802 - 4259]	4048 [3831 - 4264]	4068 [3860 - 4275]	3967 [3775 - 4157]	3992 [3748 - 4111]
1:200-year ARI						
RCP 2.6	4551 [4263 - 4839]	4544 [4274 - 4813]	4410 [4165 - 4654]	4376 [4145 - 4606]	4347 [4129 - 4563]	4256 [4053 - 4458]
RCP 4.5	4477 [4192 - 4761]	4426 [4162 - 4689]	4274 [4037 - 4511]	4201 [3981 - 4419]	4091 [3889 - 4291]	4104 [3908 - 4299]
RCP 6.0	4376 [4098 - 4652]	4265 [4013 - 4517]	4247 [4044 - 4482]	4281 [4055 - 4506]	4149 [3943 - 4354]	4234 [4030 - 4437]
RCP 8.5	4469 [4189 - 4748]	4438 [4178 - 4696]	4458 [4212 - 4702]	4482 [4246 - 4717]	4368 [4151 - 4584]	4397 [4186 - 4606]

FFA analysis across all radiative forcing scenarios for the different return period indicates:

- 1:50-year ARI future flood frequency characteristics are peaking by the 2040's under lowest radiative forcing pathways, while slightly decreasing with time. Under increased warming 1:50 year ARI flood characteristics are peaking around the 2070s and remain relatively stable for future time periods.

- 1:100 and 1:200-year ARI flood characteristics are peaking by the 2040s while slightly decreasing with time across independently of radiative forcing pathways. The result seems to indicate a change in the frequency of more extreme event with time across all radiative forcing pathways.

- Considering uncertainty, flood characteristics across future time slice and warming scenarios remain stable within 95th percentile uncertainty bands.

- Future flood frequency characteristics tends to be lower than hindcast characteristics (including 95th percentile uncertainty bounds), indicating that current level of flood risk at Anzac Parade is unlikely to change (based on the analysis taking into account the full range of the annual peak discharge time series (i.e., starting in 1986)).

5.2.5   Change in frequency of flood event under warming scenarios

For assessment of climate change impact on flood characteristics, we need to consider the potential change in peak discharge for a specific return period event (as done in this study) and change in the frequency of flood events (not addressed in this study). Both changes in amplitude and frequency impact flood frequency characteristics. Change in frequency is usually performed using peak over threshold method (POT). To illustrate how climate change is likely to impact change in frequency of flood event, Figure 5-4 to Figure 5-6 present, for each GCM and each radiative forcing scenario and over the period 2006–2098, the timing and amplitude of flood event above the GCM driven hindcast Mean Annual Flood (MAF) characteristic.

Analysis of the GCM specific, number of peaks over the GCM driven hindcast MAF indicates that:

- The timing and amplitude of flood events larger than hindcast GCM driven MAF is GCM specific.

- Generally, there is an increase (across all GCMs) in the number of flood events larger than MAF with radiative forcing pathway and time.
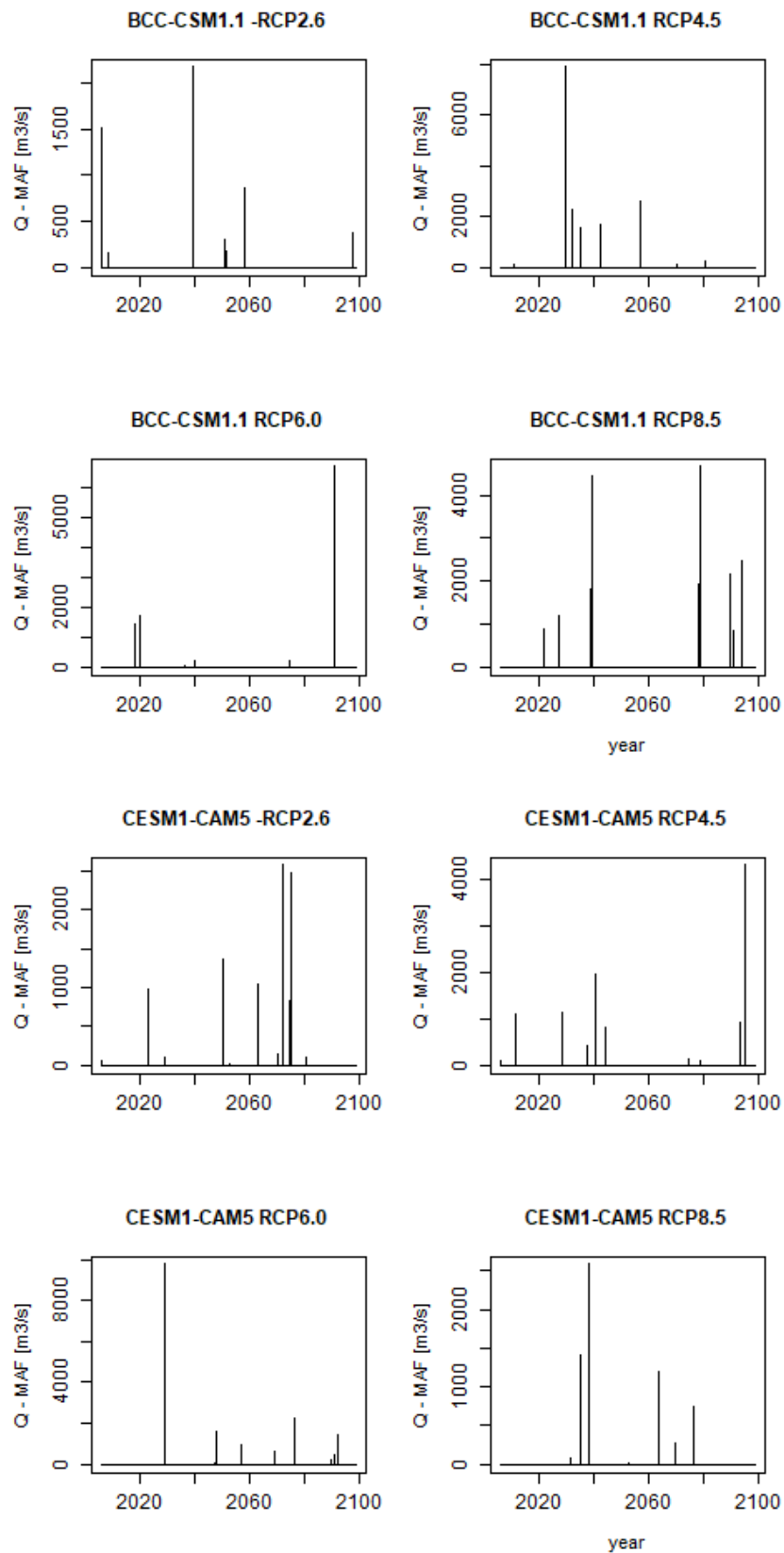
Figure 5-4: Future annual time series of GCM driven discharge above historical GCM MAF over the period 2006-2098 and across radiative forcing scenarios for BCC-CXM1.1 and CESM1-CAM5 GCMs.
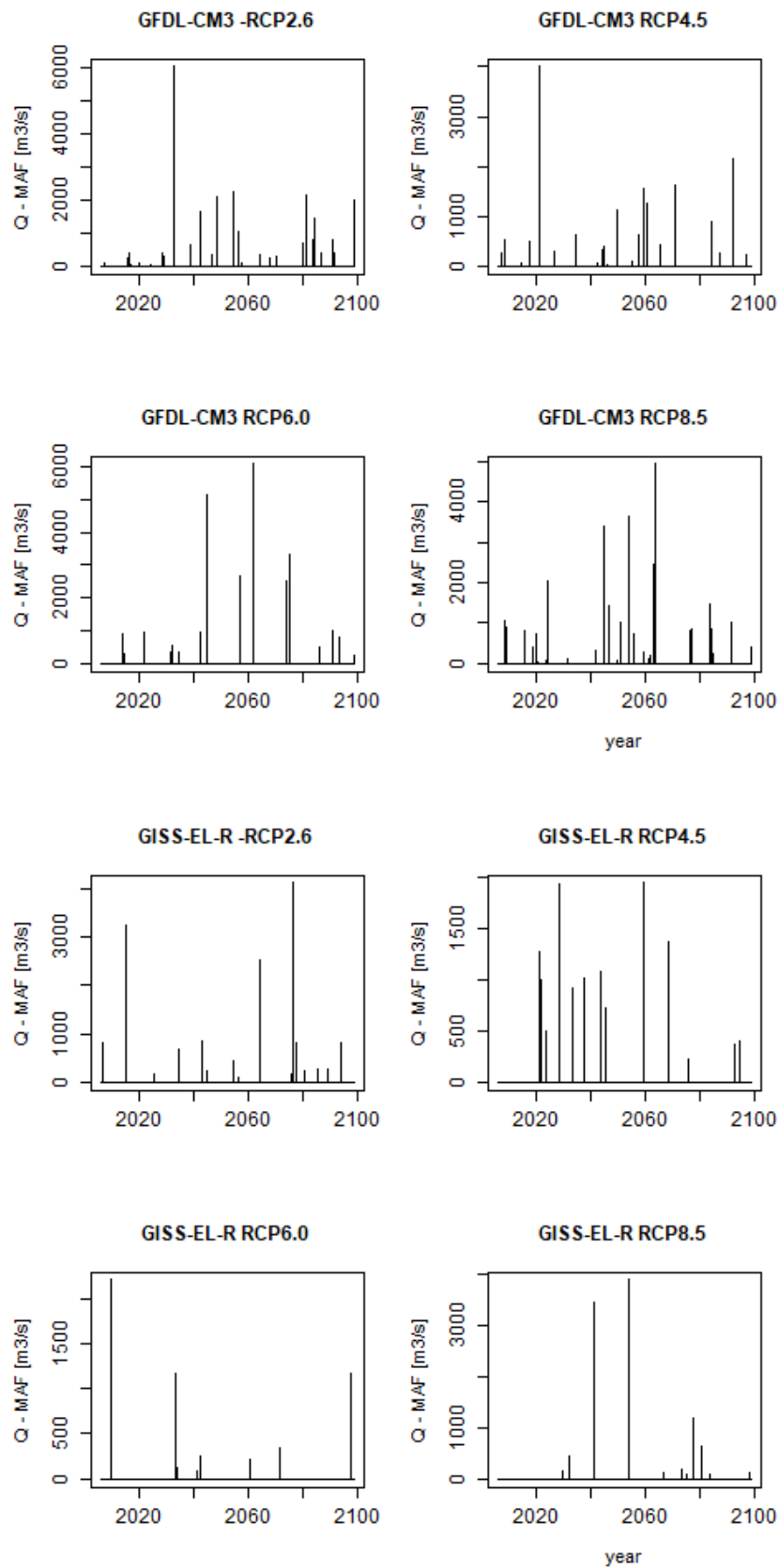
Figure 5-5: Future annual time series of GCM driven discharge above historical GCM MAF over the period 2006-2098 and across radiative forcing scenarios for GFDL-CM3 and GISS-EL-R GCMs

Climate change impact on peak discharge characteristics of the Whanganui River at Anzac Parade
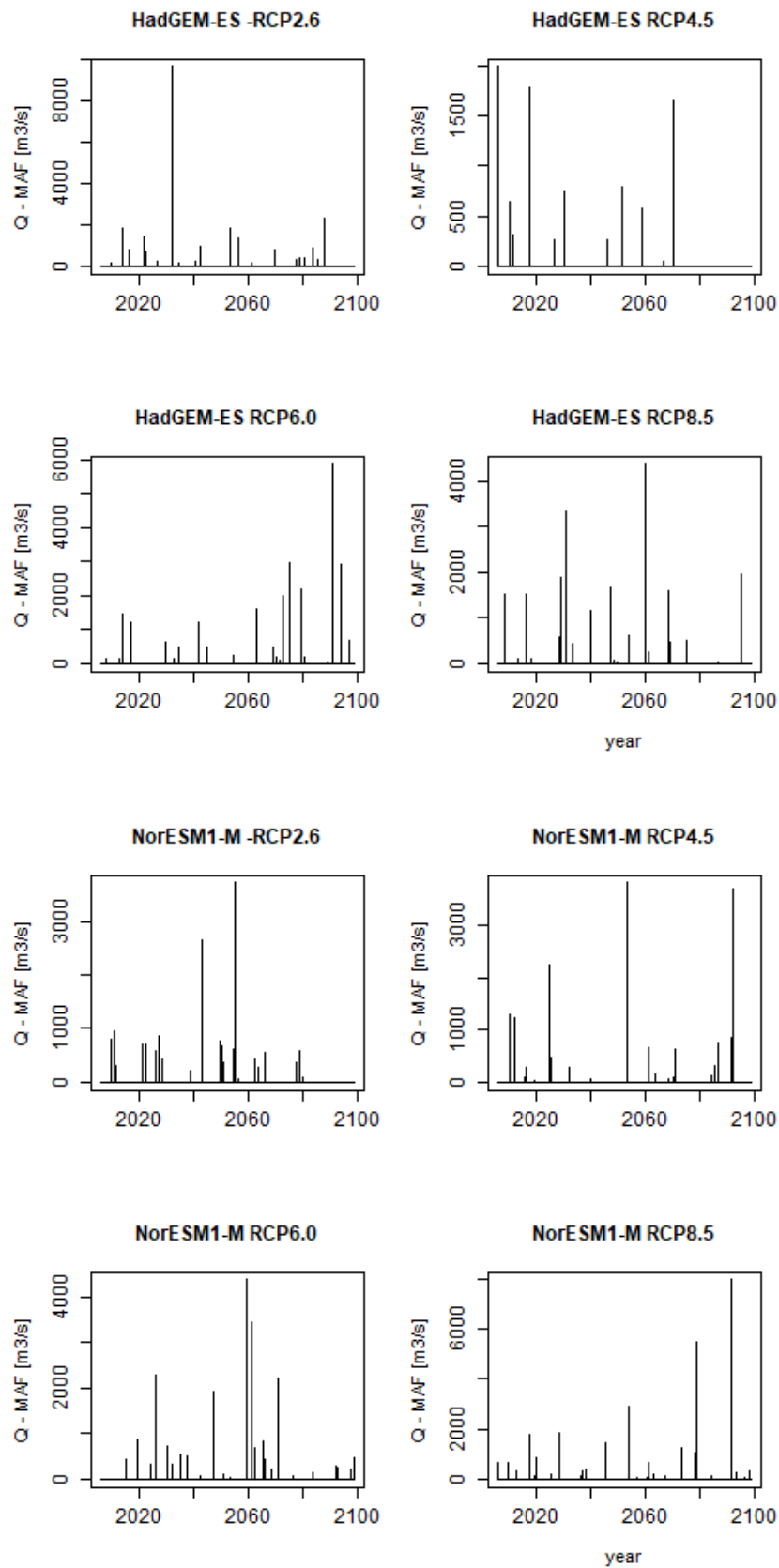
Figure 5-6: Future annual time series of GCM driven discharge above historical GCM MAF over the period 2006-2098 and across radiative forcing scenarios for HadGEM-ES and NorESM10-M GCMs.

---

6 Limitations and application of this work

This report documents the modelled changes in Whanganui River flood characteristics at Anzac Parade only. The hydrological model used as part of this investigation is uncalibrated. As a result, the modelled hydrological fluxes might not be representative of measured fluxes upstream of Anzac Parade in the Whanganui River catchment (not investigated as part of this project).

The following limitations, which apply to the national scale modelling completed to date and also apply to the analysis provided in this project:

- The TopNet hydrological model is a catchment-scale surface water model with a simplified description of catchment scale groundwater processes and conceptualisation.

- Analysis is available only for the IPCC 5th Assessment- referred hereafter as CMIP5 projections (information associated with IPCC 6th Assessment is not available before 2024).

- The TopNet hydrological model is uncalibrated and parametrisation (hydrology and climate parameters) is based on national available datasets, without fine tuning of those parameters at the regional or catchment scale.

- CMIP5 climate models are "free running" (i.e., not constrained by historical climate observations) since 1 Jan 1971 and are used as a boundary condition to a regional climate model (RCM). As a result, the RCM driven simulations are not constrained to match climate observations over the hindcast period (i.e., 1985–2006).

- CMIP5 RCM simulation is bias corrected to ERA5[5] observations (at 29 km spatial resolution) and dynamically downscaled to the Virtual Climate Station Network (VCSN) for precipitation and temperature (see Sood 2014 for technical information). As a result, any current bias in the VCSN climate observation is present in the CMIP5 climate hindcast simulations.

- The coupled CMIP5-hydrology model has been bias corrected for **water balance only** (i.e., not targeting low flow nor high flows but average flows) for the average 6 GCMs not specifically for each GCM. The bias correction is using the same methodology as developed by Woods et al. (2006).

- Validation of the CMIP5 driven national model (taken as the median across the six GCMs) has been carried out by comparison of hydrological characteristics calculated over ~400 natural streamflow stations in New Zealand. Based on Collins (2020). Figure 6-1 presents the validation of high flow hydrological characteristics, characterised as the Mean Annual Flood (MAF), across New Zealand over the period 1986–2005.

---

[5] ERA5 is a comprehensive reanalysis, from 1979 (soon to be backdated to 1950) to near real time, which assimilates as many observations as possible in the upper air and near surface. The ERA5 atmospheric model is coupled with a land surface model and a wave model. ERA5 is produced using 4D-Var data assimilation and model forecasts in CY41R2 of the European Centre for Medium-Range Weather Forecasts (ECMWF) Integrated Forecast System (IFS), with 137 hybrid sigma/pressure (model) levels in the vertical and the top level at 0.01 hPa.
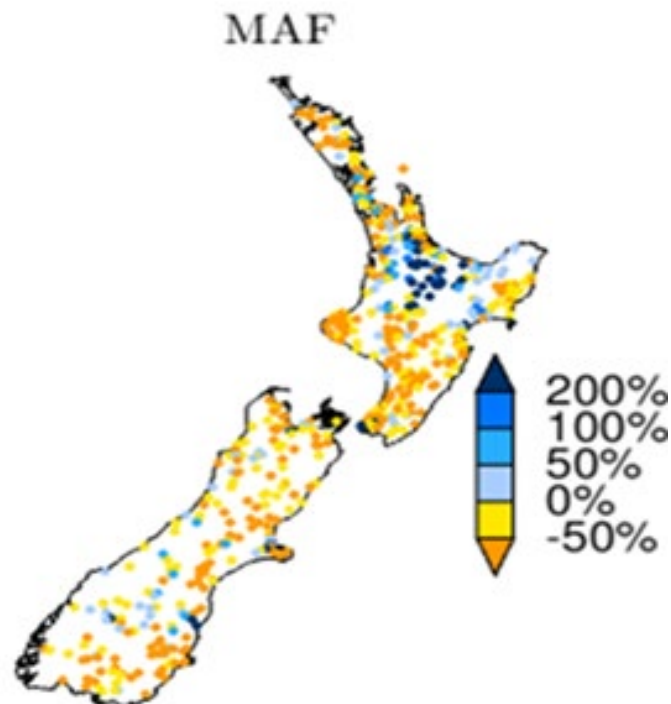
Figure 6-1: Spatial distribution of the percentage bias (Pbias) between observed and simulated Mean Annual Flood (MAF) over the period 1986–2005 (Collins 2020).

- No bias correction (either through the model or through post-processing was carried out for "future" time periods, i.e., 2006 onwards) to match observed hydrological characteristics over the period 2006–2020.

- Analysis of hydrological characteristics is available only at daily time steps as climate projections are provided at a daily time step, which could be a limiting factor for flood analysis.

- Simulations are available on Digital River Network version 2.3 (DN2v3) aggregated Strahler 3 reaches (the same spatial resolution than the national Flow Forecasting system used by NIWA). As a result, not every reach is represented.

- Not all climate model projections for the six GCMs are available to 2120 but are all available up to December 2098 (especially under RCP6.0).

- Any extreme analysis will be carried out assuming that the six GCMs are able to fully describe the tail end of the distributions. Other tools and climate projections are available for tail focussed distribution, but they are currently not available for HRC as part of this project.

7   Summary

NIWA carried out an assessment of the potential climate change impact on flood characteristics for the Whanganui River at Anzac Parade. The assessment used hydrological simulations completed as part of the Deep South National Climate Challenge's Climate change impact on National Hydrology project which couples NIWA climate change projections (Ministry for the Environment 2018) with NIWA's national hydrological modelling tool (TopNet). The modelling completed considers the impacts of climate change only with all other hydrological parameters and inputs remaining invariant through time.

Future frequency analysis characteristics were estimated using three methods (referred hereafter as FFA method):

- 20-year centred analysis comparison with flood frequency analysis carried out over a reference period (1986–2005). This method is aligned with previous regional scale climate change impact assessments.

- Future flood frequency analysis carried out on all future (as defined by IPCC 5th Assessment) time periods starting from 2006 and compared to FFA carried out over a reference period (1986–2005).

- Future flood frequency analysis carried out on available information starting from 2006 and compared to flood frequency analysis carried out over a reference period (1986–2005). This method aligns with the current practice in place within regional councils.

Analysis was carried out for each GCM used as part of the NIWA Climate change projection (six GCMs) as well as for the pooled GCMs, with the latter expected to have lower uncertainty bounds associated with predicted flood peak magnitude.

Future flood frequency analysis for the Whanganui River at Anzac Parade indicates that:

- The FFA methods used to characterise future flood peak magnitude (as described above) influence the determination of the magnitude of the peak discharge characterising specific annual return interval event. However, the choice of the method does not seem to impact the outcome of the analysis.

- Uncertainty in estimating the climate change impacts on the extreme events in the Whanganui River is large and independent of the FFA method used to characterise flood peak magnitude. The largest uncertainty is for the reference period.

- Analysis of the flood peaks from 2030 out to 2089 indicates that there could be little change in the magnitude of the 50, 100, and 200-year ARI events, but an increased frequency of flood events above MAF with time.

- Flood peaks tend to exhibit little change across the future time period independently of time period considered and radiative forcing pathways. This indicates that, within current uncertainty characterisation, current flood characteristics estimated on existing long record are expected to remain relatively stable for the foreseeable future.

- More work is required in the future to quantify the impacts of climate change on extreme flood events in this catchment using climate projection ensemble currently

being developed as part of IPCC 6th Assessment application to New Zealand (available by end of 2024) and/or Whakahura MBIE research program (available by end of 2023).

8   References

Bandaragoda, C., Tarboton, D.G., Woods, R.A. (2004) Application of TopNet in the distributed model intercomparison project. *J. Hydrol.*, 298:178-201.

Bentsen, M., (2013) The Norwegian Earth System Model, NorESM1-M - Part 1: Description and basic evaluation of the physical climate. Geosci. Model Dev., 6, 687-720. https://doi.org/10.5194/gmd-6-687-2013

Beven, K.J., Lamb, R., Quinn, P., Romanowicz, R., Freer, J. (1995) TOPMODEL. In: *Computer Models of Watershed Hydrology*, edited by: Singh, V.P., Water Resour. Publ., Highlands Ranch, Colorado, 627-668.

Clark, M.P., Rupp, D.E., Woods, R.A., Zheng, X., Ibbitt, R.P., Slater, A.G., Schmidt, J., Uddstrom, M.J. (2008) Hydrological data assimilation with the ensemble Kalman filter: Use of streamflow observations to update states in a distributed hydrological model. *Advances in Water Resources*, 31(10): 1309-1324. 10.1016/j.advwatres.2008.06.005

Collins, D.B.G., Woods, R.A., Rouse, H., Duncan, M., Snelder, T., Cowie, B. (2012) Chapter 8 Water Resources: Water resource impacts and adaptation under climate change. *Impacts of Climate Change on Land-based Sectors and Adaptation Options. Technical Report to the Sustainable Land Management and Climate Change Adaptation Technical Working Group*: p. 347-386.

Collins, D. (2013) *Mean annual river flows across New Zealand under climate change*. Paper presented at the New Zealand Hydrological Society Conference, Palmerston North.

Collins, D. (2016) Physical changes to New Zealand's freshwater ecosystems under climate change. *Freshwater conservation under a changing climate*, Wellington.

Collins, D., Zammit, C. (2016) Climate change impacts on agricultural water resources and flooding. *NIWA Client Report No. 2016114CH*: 71.

Destremau, K., Siddharth, P. (2018) How does the dairy sector share its growth- an analysis of the flow-on benefits of dairy's revenue generation? NZIER final report to Dairy Companies Association of New Zealand: 44 pp.

Goring, D.G. (1994) Kinematic shocks and monoclinal waves in the Waimakariri, a steep, braided, gravel-bed river. *Proceedings of the International Symposium on Waves: Physical and Numerical Modelling*, University of British Columbia, Vancouver, Canada, 21-24 August 1994, pp. 336-345.

Griffies, S. M. (2011) The GFDL CM3 Coupled Climate Model: Characteristics of the Ocean and Sea Ice Simulations, Journal of Climate, 24(13), 3520-3544. https://journals.ametsoc.org/view/journals/clim/24/13/2011jcli3964.1.xml

Harrington, L., Rosier, S., Dean, S.M., Stuart, S., Scahill, A. (2014) The role of anthropogenic climate change in the 2013 drought over North Island, New Zealand. *Bulletin of the American Meteorological Society*, 95(9): S45-S48.

Hawkins, E., Sutton, R. (2012) Time of emergence of climate signals. *Geophysical Research Letters, 39*. doi:Artn L0170210.1029/2011gl050087.

Ibbitt, R.P., Woods, R. (2002) Towards rainfall-runoff models that do not need calibration to flow data, in: Friend 2002 - Regional Hydrology: Bridging the Gap Between Research and Practice, edited by: van Lanen, H. A. J. and Demuth, S., IAHS Publ., 274, 189-196.

IPCC (2014) Climate Change 2014: Synthesis Report. Contribution of Working Groups I, II and III to the Fifth Assessment Report of the Intergovernmental Panel on Climate Change: 151 pp.

Jones, C. D. (2011) The HadGEM2-ES implementation of CMIP5 centennial simulations. Geosci. Model Dev., 4, 543-570. https://doi.org/10.5194/gmd-4-543-2011

Lawrence, J., Haasnoot, M., McKim, L., Atapattu, D., Campbell, G., Stroombergen, A. (2019) Dynamic Adaptive Policy Pathways (DAPP): From Theory to Practice. In: V.A.W.J. Marchau, W.E. Walker, P.J.T.M. Bloemen & S.W. Popper (Eds). *Decision Making under Deep Uncertainty: From Theory to Practice*. Springer International Publishing, Cham: 187-199. 10.1007/978-3-030-05252-2_9

McMillan, H., Clark, M., Bowden, W.B., Duncan, M.J., Woods, R. (2011) Hydrological field data from a modeller's perspective. Part 1: diagnostic tests for model structure. *Hydrol. Process*. 25 (4), 511-522.

McMillan, H.K., Hreinsson, E.O., Clark, M.P., Singh, S.K., Zammit, C., Uddstrom, M.J. (2013) Operational hydrological data assimilation with the recursive ensemble Kalman Filter. *Hydrol. Earth Syst. Sci.*, 17, 21-38.

McMillan, H.K., Booker, D.J., Cattoen, C. (2016) Validation of a national hydrological model. *Journal of Hydrology*, 541: 800-815. 10.1016/j.jhydrol.2016.07.043.

Meehl, G. A. (2013) Climate Change Projections in CESM1(CAM5) Compared to CCSM4, Journal of Climate, 26(17), 6287-6308. https://journals.ametsoc.org/view/journals/clim/26/17/jcli-d-12-00572.1.xml

Ministry for the Environment (2008) Proposed National Environmental Standard on Ecological Flows and Water Levels. Ministry for the Environment, Wellington, 61 pp.

Ministry for the Environment (2010) Tools for estimating the effects of climate change on flood flow: A guidance manual for local government in New Zealand. Ministry for the Environment, Wellington, 63 pp.

Ministry for the Environment. (2014) *National Policy Statement for Freshwater Management*. Wellington, p. 31.

Ministry for the Environment (2018) Climate Change Projections for New Zealand: Atmosphere Projections Based on Simulations from the IPCC Fifth Assessment, 2nd edition. Wellington. Ministry for the Environment, Wellington, 131 pp.

Mullan, A. B., Stuart, S. J., Hadfield, M. G., Smith, M. J. (2010) *Report on the Review of NIWA's 'Seven-Station' Temperature Series*. NIWA Information Series No. 78. Wellington, p. 55.

Newsome, P.F.J., Wilde, R.H., Willoughby, E.J. (2000) Land Resource Information System Spatial Data Layers, Technical Report, Palmerston North, Landcare Research NZ Ltd., New Zealand.

Schmidt, G. A. (2014) Configuration and assessment of the GISS ModelE2 contributions to the CMIP5 archive, J. Adv. Model. Earth Syst., 6, 141- 184. https://doi.org/10.1002/2013MS000265

Snelder, T.H., Biggs, B.J.F. (2002) Multiscale river environment classification for water resources management. *Journal of the American Water Resources Association*, 38:1225-1239.

Sood, A. (2014) Improved bias corrected and downscaled regional climate model data for climate impact studies: Validation and assessment for New Zealand. Retrieved from *www.researchgate.net/publication/265510643_Improved_Bias_Corrected_and_Downscaled_Regional_Climate_Model_Data_for_Climate_Impact_Studies_Validation_and_Assessment_for_New_Zealand*.

Woods, R. A., Hendrikx, J., Henderson, R., Tait, A. (2006). Estimating the mean flow of New Zealand rivers. Journal of Hydrology (New Zealand), 54(2), 95-110.

Wu, T. (2014) An overview of BCC climate system model development and application for climate change studies. Journal of Meteorological Research, 28, 34-56. https://doi.org/10.1007/s13351-014-3041-7

Appendix A   Flood Frequency over 20 years centred period

Table A-1:   **20 years GCM FFA analysis and associated 95th percentile uncertainty for RCP2.6 over the period 2040s–2090s.** FFA calculated on annual peak discharge (m3/s) over 20 years' time period centred on the period of interest.

	Return period					
	2030-2049	**2040-2059**	**2050-2069**	**2060-2079**	**2070-2089**	**2080-2098**
1:50-year ARI						
HadGEM2-ES	4669	3529	3064	2812	3552	3361
CESM1-CAM5	2016	2600	2808	3789	3753	2215
GFDL-CM3	4429	4034	3258	2736	3375	4117
GISS-EL-R	3041	3137	3203	3991	3988	3190
BCC-CSM1.1	3261	3150	2830	2008	2076	2491
NorESM1-M	2989	3895	3568	2907	2803	2745
Ensemble	3420	3417	3190	3030	3315	3015
1:100-year ARI						
HadGEM2-ES	5287	3944	3385	3082	3921	3722
CESM1-CAM5	2197	2871	3110	4250	4197	2415
GFDL-CM3	4991	4534	3629	3010	3742	4608
GISS-EL-R	3362	3474	3552	4473	4464	3540
BCC-CSM1.1	3630	3509	3144	2197	2269	2731
NorESM1-M	3310	4369	3977	3211	3108	3037
Ensemble	3820	3813	3546	3360	3687	3338
1:200-year ARI						
HadGEM2-ES	5903	4358	3704	3350	4290	4081
CESM1-CAM5	2377	3141	3411	4709	4638	2614
GFDL-CM3	5550	5033	3998	3283	4108	5097
GISS-EL-R	3682	3809	3900	4954	4938	3889
BCC-CSM1.1	3999	3867	3456	2386	2460	2971
NorESM1-M	3629	4841	4385	3515	3413	3328
Ensemble	4219	4209	3900	3690	4058	3661

Table A-2:   20 years GCM FFA analysis and associated 95th percentile uncertainty for RCP4.5 over the period 2040s-2090s. FFA calculated on annual peak discharge (m³/s) over 20 years' time period centred on the period of interest.

	Return period					
	2030-2049	2040-2059	2050-2069	2060-2079	2070-2089	2080-2098
1:50-year ARI						
HadGEM2-ES	2231	2536	2585	2550	2481	2061
CESM1-CAM5	2785	2477	2139	2631	2387	3207
GFDL-CM3	2553	3403	3507	3019	2896	3629
GISS-EL-R	3593	3294	3190	2982	2734	2663
BCC-CSM1.1	5501	3248	2711	2255	2574	2406
NorESM1-M	2564	2799	3042	2940	3019	3438
Ensemble	3201	3102	2921	2764	2729	2941
1:100-year ARI						
HadGEM2-ES	2445	2789	2841	2804	2742	2259
CESM1-CAM5	3112	2755	2349	2908	2643	3598
GFDL-CM3	2809	3771	3884	3339	3191	4034
GISS-EL-R	4009	3653	3550	3322	3024	2936
BCC-CSM1.1	6251	3646	3004	2453	2828	2645
NorESM1-M	2816	3075	3373	3258	3342	3824
Ensemble	3572	3452	3239	3055	3017	3266
1:200-year ARI						
HadGEM2-ES	2658	3041	3095	3056	3003	2457
CESM1-CAM5	3437	3032	2559	3183	2897	3987
GFDL-CM3	3064	4137	4259	3657	3484	4438
GISS-EL-R	4425	4011	3909	3662	3314	3208
BCC-CSM1.1	6999	4043	3295	2651	3080	2883
NorESM1-M	3067	3351	3704	3575	3663	4209
Ensemble	3942	3801	3554	3346	3305	3590

Table A-3:   20 years GCM FFA analysis and associated 95th percentile uncertainty for RCP 6.0 over the period 2040s–2090s.   FFA calculated on annual peak discharge (m^3/s) over 20 years' time period centred on the period of interest.

	Return period					
	2030-2049	**2040-2059**	**2050-2069**	**2060-2079**	**2070-2089**	**2080-2098**
1:50-year ARI						
HadGEM2-ES	3115	2652	2619	4591	4178	4471
CESM1-CAM5	2698	2813	2653	3054	3066	2986
GFDL-CM3	3629	3967	3861	4334	3223	2941
GISS-EL-R	2837	2281	2371	2523	3066	2675
BCC-CSM1.1	2683	2702	2658	2869	2643	3907
NorESM1-M	3294	3455	4388	3871	2520	2493
Ensemble	3105	3010	3100	3547	3066	3260
1:100-year ARI						
HadGEM2-ES	3459	2937	2899	5158	4663	5008
CESM1-CAM5	2997	3125	2930	3388	3405	3314
GFDL-CM3	4052	4439	4327	4893	3606	3265
GISS-EL-R	3144	2501	2596	2731	3405	2949
BCC-CSM1.1	2936	2978	2920	3163	2921	4383
NorESM1-M	3650	3860	4929	4326	2774	2740
Ensemble	3446	3344	3444	3953	3404	3628
1:200-year ARI						
HadGEM2-ES	3801	3221	3177	5723	5147	5543
CESM1-CAM5	3294	3435	3206	3721	3744	3642
GFDL-CM3	4473	4909	4790	5451	3989	3587
GISS-EL-R	3450	2720	2822	2938	3744	3222
BCC-CSM1.1	3188	3252	3181	3457	3198	4857
NorESM1-M	4004	4263	5469	4780	3027	2985
Ensemble	3787	3678	3788	4358	3740	3994

Table A-4: **20 years GCM FFA analysis and associated 95th percentile uncertainty for RCP8.5 over the period 2040s–2090s.** FFA calculated on annual peak discharge (m^3/s) over 20 years' time period centred on the period of interest.

	Return period					
	2030-2049	2040-2059	2050-2069	2060-2079	2070-2089	2080-2098
1:50- year ARI						
HadGEM2-ES	3920	3383	4051	3847	2406	2794
CESM1-CAM5	3417	2405	3155	3312	2263	2201
GFDL-CM3	3333	4566	4883	4097	3225	3221
GISS-EL-R	3295	4143	3535	3592	3522	3299
BCC-CSM1.1	3081	2163	2120	3259	4046	3817
NorESM1-M	3045	3089	3102	3668	3599	4036
Ensemble	3402	3332	3574	3754	3229	3235
1:100- year ARI						
HadGEM2-ES	4373	3763	4552	4316	2641	3089
CESM1-CAM5	3815	2655	3509	3695	2493	2410
GFDL-CM3	3725	5119	5474	4571	3580	3576
GISS-EL-R	3661	4617	3905	3968	3888	3655
BCC-CSM1.1	3425	2363	2324	3655	4559	4282
NorESM1-M	3392	3424	3420	4057	4006	4524
Ensemble	3794	3709	3985	4194	3592	3599
1:200- year ARI						
HadGEM2-ES	4824	4142	5050	4783	2875	3384
CESM1-CAM5	4211	2905	3862	4077	2723	2619
GFDL-CM3	4115	5671	6063	5043	3933	3929
GISS-EL-R	4025	5090	4273	4343	4253	4009
BCC-CSM1.1	3768	2562	2527	4049	5071	4746
NorESM1-M	3738	3757	3737	4444	4411	5011
Ensemble	4186	4084	4394	4632	3954	3962

Appendix B   Flood Frequency Analysis on future period - 2006 FFA

Table B-1:   2006 GCM FFA analysis and associated 95th percentile uncertainty for RCP2.6 over the period 2040s–2090s. FFA calculated on annual peak discharge (m^3/s) over time periods starting in 2006.

	Return period					
	2030-2049	**2040-2059**	**2050-2069**	**2060-2079**	**2070-2089**	**2080-2098**
1:50-year ARI						
HadGEM2-ES	4067	3971	3841	3718	3810	3658
CESM1-CAM5	2176	2370	2396	2744	2735	2649
GFDL-CM3	3530	3583	3493	3383	3487	3526
GISS-EL-R	3215	3185	3250	3402	3434	3366
BCC-CSM1.1	3038	3171	2971	2829	2762	2786
NorESM1-M	3207	3390	3332	3261	3225	3158
Ensemble	3277	3338	3253	3258	3267	3210
1:100-year ARI						
HadGEM2-ES	4561	4448	4296	4150	4252	4077
CESM1-CAM5	2397	2619	2647	3050	3037	2935
GFDL-CM3	3937	4002	3896	3768	3886	3932
GISS-EL-R	3566	3531	3607	3784	3820	3742
BCC-CSM1.1	3381	3533	3305	3140	3063	3088
NorESM1-M	3551	3768	3698	3619	3580	3504
Ensemble	3651	3721	3622	3628	3636	3570
1:200-year ARI						
HadGEM2-ES	5053	4923	4749	4580	4693	4495
CESM1-CAM5	2617	2867	2898	3355	3337	3221
GFDL-CM3	4342	4420	4298	4151	4283	4336
GISS-EL-R	3915	3876	3962	4165	4205	4118
BCC-CSM1.1	3722	3893	3637	3451	3363	3388
NorESM1-M	3893	4144	4063	3976	3934	3848
Ensemble	4024	4102	3989	3996	4003	3929

Table B-2: 2006 GCM FFA analysis and associated 95th percentile uncertainty for RCP4.5 over the period 2040s–2090s. FFA calculated on annual peak discharge (m^3/s) over time periods starting in 2006.

	Return period					
	2030-2049	2040-2059	2050-2069	2060-2079	2070-2089	2080-2098
1:50-year ARI						
HadGEM2-ES	2780	2844	2728	2761	2677	2618
CESM1-CAM5	2974	2796	2708	2723	2641	2832
GFDL-CM3	2984	3154	3165	3115	3103	3219
GISS-EL-R	3707	3637	3545	3478	3370	3343
BCC-CSM1.1	3653	3617	3348	3266	3179	3079
NorESM1-M	2876	2940	2942	2954	2957	3055
Ensemble	3193	3206	3108	3078	3013	3051
1:100-year ARI						
HadGEM2-ES	3078	3150	3014	3053	2959	2892
CESM1-CAM5	3312	3111	3005	3023	2930	3152
GFDL-CM3	3307	3498	3509	3452	3436	3570
GISS-EL-R	4129	4051	3948	3877	3750	3721
BCC-CSM1.1	4099	4058	3743	3645	3544	3428
NorESM1-M	3168	3242	3249	3263	3268	3381
Ensemble	3553	3568	3454	3420	3344	3389
1:200-year ARI						
HadGEM2-ES	3375	3455	3299	3343	3240	3164
CESM1-CAM5	3649	3424	3302	3322	3218	3471
GFDL-CM3	3628	3840	3851	3788	3767	3920
GISS-EL-R	4549	4463	4351	4274	4128	4098
BCC-CSM1.1	4543	4498	4138	4023	3908	3775
NorESM1-M	3459	3543	3555	3572	3578	3705
Ensemble	3911	3929	3799	3760	3674	3726

Table B-3: **2006 GCM FFA analysis and associated 95th percentile uncertainty for RCP 6.0 over the period 2040s–2090s.** FFA calculated on annual peak discharge (m^3/s) over time periods starting in 2006.

	Return period					
	2030-2049	**2040-2059**	**2050-2069**	**2060-2079**	**2070-2089**	**2080-2098**
1:50-year ARI						
HadGEM2-ES	3125	2953	2985	3369	3321	3647
CESM1-CAM5	3108	3016	2946	3049	3003	3042
GFDL-CM3	3032	3113	3283	3368	3290	3307
GISS-EL-R	2730	2580	2608	2673	3003	2672
BCC-CSM1.1	3039	2942	2920	2921	2877	3114
NorESM1-M	3201	3290	3537	3453	3334	3291
Ensemble	3052	3007	3067	3158	3067	3179
1:100-year ARI						
HadGEM2-ES	3463	3271	3309	3751	3693	4070
CESM1-CAM5	3474	3365	3281	3399	3344	3389
GFDL-CM3	3366	3457	3656	3757	3670	3687
GISS-EL-R	3021	2850	2877	2948	3344	2946
BCC-CSM1.1	3371	3261	3231	3234	3185	3458
NorESM1-M	3565	3671	3951	3855	3717	3667
Ensemble	3393	3341	3408	3512	3407	3537
1:200-year ARI						
HadGEM2-ES	3799	3588	3632	4132	4064	4491
CESM1-CAM5	3839	3714	3615	3747	3684	3734
GFDL-CM3	3698	3800	4028	4144	4048	4066
GISS-EL-R	3311	3119	3145	3222	3684	3219
BCC-CSM1.1	3703	3578	3540	3545	3491	3801
NorESM1-M	3928	4050	4364	4256	4099	4041
Ensemble	3732	3675	3748	3866	3746	3893

Table B-4: **2006 GCM FFA analysis and associated 95th percentile uncertainty for RCP8.5 over the period 2040s–2090s.** FFA calculated on annual peak discharge (m^3/s) over time periods starting in 2006.

	Return period					
	2030-2049	**2040-2059**	**2050-2069**	**2060-2079**	**2070-2089**	**2080-2098**
1:50- year ARI						
HadGEM2-ES	3659	3501	3814	3657	3510	3474
CESM1-CAM5	2775	2717	2889	2893	2752	2749
GFDL-CM3	3573	3775	3978	3863	3806	3731
GISS-EL-R	2790	3132	3096	3269	3224	3277
BCC-CSM1.1	2999	2856	2715	2965	2987	3156
NorESM1-M	3368	3382	3317	3523	3402	3620
Ensemble	3228	3263	3339	3396	3312	3361
1:100- year ARI						
HadGEM2-ES	4067	3891	4258	4078	3911	3870
CESM1-CAM5	3080	3013	3208	3215	3053	3048
GFDL-CM3	3983	4215	4446	4313	4249	4162
GISS-EL-R	3081	3472	3426	3624	3569	3632
BCC-CSM1.1	3325	3162	3002	3295	3320	3517
NorESM1-M	3743	3759	3681	3916	3779	4031
Ensemble	3588	3629	3715	3782	3685	3742
1:200- year ARI						
HadGEM2-ES	4474	4279	4700	4498	4309	4264
CESM1-CAM5	3384	3307	3527	3536	3353	3346
GFDL-CM3	4391	4654	4911	4761	4689	4591
GISS-EL-R	3370	3811	3755	3977	3912	3986
BCC-CSM1.1	3650	3466	3289	3624	3651	3877
NorESM1-M	4117	4135	4043	4307	4154	4441
Ensemble	3947	3993	4090	4166	4056	4121

Appendix C   Flood Frequency Analysis on longest time record - 1986 FFA

Table C-1:   1986 GCM FFA analysis and associated 95th percentile uncertainty for RCP2.6 over the period 2040s–2090s. FFA calculated on annual peak discharge (m^3/s) over time periods starting in 1986.

	Return period					
	2030-2049	**2040-2059**	**2050-2069**	**2060-2079**	**2070-2089**	**2080-2098**
1:50-year ARI						
HadGEM2-ES	4209	4126	3971	3856	3910	3782
CESM1-CAM5	3143	3173	3097	3273	3205	3125
GFDL-CM3	3578	3628	3521	3432	3497	3530
GISS-EL-R	3793	3701	3666	3735	3728	3691
BCC-CSM1.1	3854	3894	3676	3497	3358	3321
NorESM1-M	3337	3441	3399	3347	3294	3237
Ensemble	3705	3696	3591	3564	3542	3472
1:100-year ARI						
HadGEM2-ES	4709	4613	4435	4300	4359	4212
CESM1-CAM5	3501	3534	3447	3651	3570	3479
GFDL-CM3	3975	4038	3915	3813	3887	3926
GISS-EL-R	4216	4113	4075	4157	4149	4109
BCC-CSM1.1	4313	4359	4112	3907	3747	3702
NorESM1-M	3687	3813	3765	3709	3651	3586
Ensemble	4129	4121	4001	3971	3945	3865
1:200-year ARI						
HadGEM2-ES	5207	5099	4897	4741	4807	4642
CESM1-CAM5	3857	3894	3796	4027	3934	3831
GFDL-CM3	4370	4447	4308	4192	4275	4321
GISS-EL-R	4638	4523	4482	4578	4569	4525
BCC-CSM1.1	4770	4823	4547	4316	4135	4081
NorESM1-M	4035	4184	4129	4069	4007	3935
Ensemble	4551	4544	4410	4376	4347	4256

Table C-2: **20 years GCM FFA analysis and associated 95th percentile uncertainty for RCP4.5 over the period 2040s–2090s.** FFA calculated on annual peak discharge (m^3/s) over time periods starting in 1986.

	Return period					
	2030-2049	2040-2059	2050-2069	2060-2079	2070-2089	2080-2098
1:50-year ARI						
HadGEM2-ES	3368	3335	3188	3167	3072	2993
CESM1-CAM5	3663	3467	3306	3256	3158	3254
GFDL-CM3	3221	3310	3312	3274	3233	3315
GISS-EL-R	4104	4051	3934	3860	3698	3662
BCC-CSM1.1	4323	4220	3948	3786	3706	3581
NorESM1-M	3097	3108	3108	3104	3085	3163
Ensemble	3649	3606	3488	3429	3344	3352
1:100-year ARI						
HadGEM2-ES	3744	3706	3537	3514	3408	3318
CESM1-CAM5	4090	3871	3685	3629	3518	3632
GFDL-CM3	3564	3664	3667	3626	3576	3672
GISS-EL-R	4568	4514	4385	4306	4118	4080
BCC-CSM1.1	4861	4745	4430	4240	4148	4003
NorESM1-M	3410	3425	3430	3428	3407	3497
Ensemble	4064	4016	3882	3816	3718	3729
1:200-year ARI						
HadGEM2-ES	4119	4076	3885	3860	3744	3642
CESM1-CAM5	4515	4275	4062	3999	3878	4008
GFDL-CM3	3905	4016	4020	3976	3918	4028
GISS-EL-R	5031	4976	4833	4750	4537	4497
BCC-CSM1.1	5396	5269	4910	4692	4589	4425
NorESM1-M	3722	3740	3751	3750	3727	3831
Ensemble	4477	4426	4274	4201	4091	4104

Table C-3: **1986 GCM FFA analysis and associated 95th percentile uncertainty for RCP 6.0 over the period 2040s–2090s.** FFA calculated on annual peak discharge (m^3/s) over time periods starting in 1986.

	Return period					
	2030-2049	**2040-2059**	**2050-2069**	**2060-2079**	**2070-2089**	**2080-2098**
1:50-year ARI						
HadGEM2-ES	3650	3623	3637	3653	3564	3585
CESM1-CAM5	3753	3620	3506	3508	3428	3427
GFDL-CM3	3247	3255	3392	3480	3394	3396
GISS-EL-R	3555	3351	3255	3220	3428	3146
BCC-CSM1.1	3865	3679	3557	3492	3389	3559
NorESM1-M	3380	3460	3605	3533	3397	3360
Ensemble	3567	3477	3464	3489	3387	3452
1:100-year ARI						
HadGEM2-ES	3897	3744	3726	4012	3946	4224
CESM1-CAM5	4201	4049	3917	3919	3826	3825
GFDL-CM3	3597	3607	3770	3875	3779	3780
GISS-EL-R	3959	3729	3614	3571	3826	3487
BCC-CSM1.1	4318	4104	3961	3888	3771	3969
NorESM1-M	3753	3851	4016	3936	3780	3737
Ensemble	3972	3872	3856	3886	3769	3844
1:200-year ARI						
HadGEM2-ES	4280	4114	4096	4420	4343	4659
CESM1-CAM5	4647	4477	4326	4328	4222	4222
GFDL-CM3	3946	3958	4146	4269	4164	4163
GISS-EL-R	4362	4106	3973	3920	4222	3827
BCC-CSM1.1	4768	4529	4364	4283	4152	4376
NorESM1-M	4126	4241	4426	4337	4162	4113
Ensemble	4376	4265	4247	4281	4149	4234

Table C-4: **1986 GCM FFA analysis and associated 95th percentile uncertainty for RCP8.5 over the period 2040s–2090s.** FFA calculated on annual peak discharge (m^3/s) over time periods starting in 1986.

	Return period					
	2030-2049	**2040-2059**	**2050-2069**	**2060-2079**	**2070-2089**	**2080-2098**
1:50- year ARI						
HadGEM2-ES	3815	3703	3925	3813	3688	3647
CESM1-CAM5	3472	3363	3396	3379	3228	3175
GFDL-CM3	3574	3765	3865	3796	3765	3712
GISS-EL-R	3500	3671	3567	3613	3570	3559
BCC-CSM1.1	3835	3609	3464	3567	3525	3651
NorESM1-M	3481	3468	3401	3525	3438	3605
Ensemble	3650	3623	3637	3653	3564	3585
1:100- year ARI						
HadGEM2-ES	4235	4112	4375	4249	4107	4061
CESM1-CAM5	3868	3745	3781	3766	3593	3531
GFDL-CM3	3966	4188	4302	4224	4191	4130
GISS-EL-R	3886	4082	3959	4011	3959	3949
BCC-CSM1.1	4284	4026	3863	3986	3937	4086
NorESM1-M	3857	3845	3766	3908	3811	4005
Ensemble	4060	4031	4048	4068	3967	3992
1:200– year ARI						
HadGEM2-ES	4653	4520	4823	4684	4525	4474
CESM1-CAM5	4262	4125	4165	4151	3957	3886
GFDL-CM3	4357	4611	4738	4651	4615	4547
GISS-EL-R	4271	4491	4350	4407	4347	4338
BCC-CSM1.1	4731	4442	4261	4403	4348	4518
NorESM1-M	4232	4220	4129	4289	4183	4403
Ensemble	4469	4438	4458	4482	4368	4397